

¹ Impacts of K-12 school reopening on the COVID-19 epidemic in ² Indiana, USA

³ Guido España[#], Sean Cavany^{*}, Rachel Oidtmann^{*}, Carly Barbera,
Alan Costello, Anita Lerch, Marya Poterek, Quan Tran, Annaliese Wieler
Sean Moore, T. Alex Perkins[#]

Department of Biological Sciences and Eck Institute for Global Health,
University of Notre Dame, United States

#Correspondence: guido.espana@nd.edu, taperkins@nd.edu

*Equal contribution

⁴ Key points

- ⁵ **Question:** What will be the impact of reopening schools on SARS-CoV-2 infections and COVID-
⁶ 19 mortality in Indiana?
- ⁷ **Findings:** Reopening schools at full capacity with low (50%) face-mask adherence could have a
⁸ substantial effect on the burden of COVID-19 across Indiana, leading to 83 times more infections
⁹ and 13 times more deaths than if schools operated remotely. Reopening at 50% capacity and
¹⁰ with 100% face-mask adherence could mitigate much of this risk, leading to 12% more infections
¹¹ and 5% more deaths than if schools operated remotely.
- ¹² **Meaning:** Schools should make efforts to reduce capacity and enforce face-mask adherence to
¹³ prevent increases in the statewide burden of COVID-19.

¹⁴ Abstract

- ¹⁵ **Importance:** In the United States, schools closed in March 2020 to reduce the burden of
¹⁶ COVID-19. They are now reopening amid high incidence in many places, necessitating analyses
¹⁷ of the associated risks and benefits.
- ¹⁸ **Objective:** To determine the impact of school reopening with varying levels of operating capacity
¹⁹ and face-mask adherence on COVID-19 burden.
- ²⁰ **Design:** Modeling study using an agent-based model that simulates daily activities of the popu-
²¹ lation. Transmission can occur in places such as schools, workplaces, community, and households.
²² Model parameters were calibrated to and validated against multiple types of COVID-19 data.
- ²³ **Setting:** Indiana, United States of America.
- ²⁴ **Participants:** Synthetic population of Indiana. K-12 students, teachers, their families, and
²⁵ others in the state were studied separately.

26 **Interventions:** Reopening of schools under three levels of school operating capacity (50%, 75%,
27 and 100%), as well as three assumptions about face-mask adherence in schools (50%, 75%, and
28 100%). We compared the impact of these scenarios to reopening at full capacity without face
29 masks and a scenario with schools operating remotely, for a total of 11 scenarios.

30 **Main outcomes:** SARS-CoV-2 infections, symptomatic cases, and deaths due to COVID-19
31 from August 24 to December 31.

32 **Results:** We projected 19,527 (95% CrI: 4,641-56,502) infections and 360 (95% CrI: 67-967)
33 deaths in the scenario where schools operated remotely from August 24 to December 31. Re-
34 opening at full capacity with low face-mask adherence in schools resulted in a proportional
35 increase of 81.7 (95% CrI: 78.2-85.3) times the number of infections and 13.4 (95% CrI: 12.8-
36 14.0) times the number of deaths. High face-mask adherence resulted in a proportional increase
37 of 3.0 (95% CrI: 2.8-3.1) times the number of infections. Operating at reduced capacity with high
38 face-mask adherence resulted in only an 11.6% (95% CrI: 5.50%-17.9%) increase in the number
39 of infections.

40 **Conclusions and Relevance:** Reduced capacity and high face-mask adherence in schools
41 would substantially reduce the burden of COVID-19 in schools and across the state. We did
42 not explore the impact of other reopening scenarios, such as alternating days of attendance.
43 Heterogeneous decisions could be made across different districts throughout the state, which our
44 model does not capture. Hence, caution should be taken in interpreting our results as specific
45 quantitative targets for operating capacity or face-mask adherence. Rather, our results suggest
46 that schools should give serious consideration to reducing capacity as much as is feasible and
47 enforcing adherence to wearing face masks.

48 1 Introduction

49 The United States has been the country most severely impacted by the COVID-19 pandemic
50 in terms of total reported cases and deaths, with over 5.2 million cases and 167,000 deaths
51 through August 14 [1]. This severity led to social interventions on an unprecedented scale,
52 including restrictions on mass gatherings, bans on non-essential travel, and school closures [2, 3,
53 4, 5]. While such restrictions were initially successful in reducing transmission, the subsequent
54 relaxation of restrictions on mass gatherings and movement were followed by large increases in
55 notified cases and, more recently, deaths [1, 3, 6, 7]. The state of Indiana reported its highest
56 daily number of cases to date (1,249) on August 6 [8].

57 It is within this context of intense community transmission that attention has turned to the
58 reopening of schools for the start of the academic year in August [9, 10, 11]. During influenza
59 epidemics, school closures have been estimated to reduce transmission community-wide [12, 13,
60 14]. In general, schools are seen as key drivers of the transmission of respiratory pathogens due to
61 close contact among children at school [15, 16, 17]. However, several factors complicate the effect
62 of school reopenings on SARS-CoV-2 transmission. In particular, children and adolescents appear
63 less susceptible to infection and are much less likely to experience severe outcomes following
64 infection [18, 19, 20, 21, 22, 23]. It is also still unclear what their contribution to transmission is,
65 but several studies suggest they can play an important role [18, 24, 25, 26]. There are additional

66 economic and social factors to consider, too, such as the economic costs of school closures for
67 families that must then stay home from work, and the nutritional benefits of school reopening
68 for children who rely on free and subsidized school meals [27, 28, 29].

69 Our objective in this study was to explore the impacts of strategies for school reopening on
70 the burden of COVID-19 in the state of Indiana, USA. We synthesized evidence around features
71 of COVID-19 epidemiology in children [19] in an agent-based model originally developed for
72 pandemic influenza [30] that is equipped to translate such evidence into projections of community-
73 wide transmission under alternative scenarios about school reopening. We focused on the role of
74 reducing the capacity of classrooms and adherence to wearing face masks in schools, given that
75 both physical distancing and face masks have been shown to reduce transmission of SARS-CoV-
76 2 in community settings [31]. Our main outcome measures were changes in statewide totals of
77 SARS-CoV-2 infections, symptomatic infections, and deaths, across different scenarios of school
78 capacity and face-mask adherence, compared with a baseline scenario in which schools operate
79 remotely.

80 2 Methods

81 Approach

82 Our approach to modeling SARS-CoV-2 transmission is based on the Framework for Recon-
83 structing Epidemic Dynamics (FRED) model [30]. Using this model, we simulated the spread of
84 SARS-CoV-2 in the population of Indiana, USA using a synthetic population with demographic
85 and geographic characteristics of the population, including age, household composition, house-
86 hold location, and occupation [32]. We analyzed the impact of school reopening from August 24
87 (first day of classes in Marion County, the most populous) to December 31, 2020 in the overall
88 population of Indiana, as well as in students, teachers, and their households. We quantified
89 impact as the difference in the number of COVID-19 infections, symptomatic infections, and
90 deaths, between each scenario and the baseline scenario.

91 Agent-based model

92 We chose an agent-based model for this analysis to address key issues such as heterogeneity of
93 transmission within a population due to population density, age, occupation, and contact net-
94 work. We used a synthetic population of Indiana to realistically represent characteristics of the
95 population [32]. FRED simulates pathogen spread in a population by recreating interactions
96 among people on a daily basis. Each human is modeled as an agent who visits a set of places
97 defined by their activity space (houses, schools, workplaces, and neighborhood locations). Trans-
98 mission can occur when an infected person visits the same location as a susceptible person on
99 the same day, with numbers of contacts per person specific to each location type. For instance,
100 school contacts depend not on the size of the school but on the age of the student. Every day of
101 the week, students and teachers visit their school, and students are assigned to classrooms based
102 on their age. Given that schools are closed during the weekends, community contact is increased
103 by 50% [30]. For both schools and other locations, we adopted contact rates for each location

104 type that were previously calibrated to attack rates for influenza specific to each location type
105 [30, 33].

106 Once infected, each individual had latent and infectious periods drawn from distributions
107 calibrated so that the average generation interval distribution matched estimates from Singapore
108 (mean = 5.20, standard deviation = 1.72) [34]. The absolute risk of transmission depended on the
109 number and location of an infected individual's contacts and a parameter that controls SARS-
110 CoV-2 transmissibility upon contact, which we calibrated. A proportion of the infections were
111 asymptomatic [35]. We assumed these infections were as infectious as symptomatic infections
112 and had identical incubation and infectious period distributions [36, 37, 26, 38]. We assumed that
113 children were less susceptible to infection than adults, which we modeled with a logistic function
114 calibrated to model-based estimates of this relationship by Davies et al. [19]. We assumed that
115 severity of disease increased with age, consistent with statistical analyses performed elsewhere
116 [39, 40, 41, 21].

117 Agent behavior in FRED has the potential to change over the course of an epidemic. Following
118 the onset of symptoms, infected agents self-isolate at home according to a fixed daily rate, whereas
119 others continue their daily activities [42, 43]. This rate was chosen so that, on average, 68% of
120 agents will self-isolate at some point during their symptoms, assuming that all individuals who
121 develop a fever will isolate at some point during their symptoms [43]. Agents can also respond
122 to public health interventions, including school closure, shelter in place, and a combination
123 of mask-wearing and social distancing. School closures occur on specific dates [44], resulting
124 in students limiting their activity space to household and neighborhood locations. Shelter-in-
125 place interventions reduce some agents' activity spaces to their households only, whereas others
126 continue with their daily routines. We used mobility reports from Google [45] to drive daily
127 compliance with shelter-in-place, such that shelter-in-place compliance in our model accounts
128 for both the effects of shelter-in-place orders and some people deciding to continue staying at
129 home after those orders are lifted [46]. We used Google Trends data for Indiana using the terms
130 "face mask" and "social distancing" [47] to capture temporal trends and survey data [48] to
131 capture the magnitude of these behaviors. Further details about the model are available in the
132 Supplementary Text.

133 Data and outcomes

134 We obtained daily incidence of death from the New York Times COVID-19 database [1]. Hospi-
135 talizations and the age distribution of deaths reported in Indiana were obtained from the Indiana
136 COVID-19 dashboard [8]. Daily numbers of tests performed in the state were available from The
137 Covid Project [49]. We calibrated the model to daily values of deaths, hospitalizations, and test
138 positivity through August 10 and to the age distribution of deaths cumulative through July 13
139 to estimate nine model parameters using a sobol design sampling algorithm [50, 51] (Supplemen-
140 tary Material). We validated the model by comparing its predictions of the infection attack rate
141 overall and by age to results from two statewide serological surveys undertaken in late April and
142 early June [52, 53].

143 To account for uncertainty in the calibrated parameters in our future projections, we sim-
144 ultated nine scenarios about school reopening with values of the model's nine free parameters

145 sampled from the calibrated distribution. From August 24 to December 31, we outputted numbers
146 of daily infections, symptomatic cases, hospitalizations, and deaths, structured by age, place
147 of infection (school, home, other), and affiliation with schools (student, teacher, none). For our
148 analysis, we focused on infections, symptomatic infections, and deaths in the overall population
149 and the subgroups of students, teachers, and their families.

150 We explored three scenarios for school operating capacity (50%, 75%, or 100% of students
151 receiving in-person instruction) and three scenarios for face-mask adherence in schools (50%, 75%,
152 or 100%). We compared each of the nine combinations of these scenarios to a scenario in which
153 schools reopened normally (100% capacity, 0% face-mask adherence) and to a scenario in which
154 schools operated remotely until the end of the calendar year. We analyzed the sensitivity of the
155 model outcomes to parameter uncertainty by calculating the partial rank correlation coefficient
156 [54] of each calibrated parameter and two outcomes: the cumulative number of infections between
157 August 24 and December 31, and the proportion of infections acquired in schools during that
158 period.

159 3 Results

160 Our model was generally consistent with the data to which it was calibrated, capturing trends
161 over time in daily deaths, hospitalizations, and test positivity (Fig. 1A-C), as well as greater
162 proportions of deaths among older age groups (Fig. 1D). Some trade-offs in the model's ability
163 to recreate different data types were apparent, such as a recent increase in hospitalizations that
164 the model failed to capture (Fig. 1C), likely due to the predominance of data on deaths in the
165 likelihood. Even so, the model's predictions reproduced the range of variability in the data,
166 as assessed by coverage probability of its 95% posterior predictive intervals (daily deaths: 0.91;
167 daily hospitalizations: 1.0; daily test positivity: 0.97; cumulative deaths by age: 1.0). The model
168 was also consistent with data withheld from fitting. Across all ages, the 95% credible intervals
169 of the cumulative proportion infected through late April (median: 0.0174; 95% CrI: 0.0058-
170 0.064) and early June (median: 0.0221; 95% CrI: 0.0072-0.08) from two state-wide serological
171 surveys [52] fell within the 95% posterior predictive intervals of our model (Fig. S1A). Our
172 model's predictions also overlapped with age-stratified estimates from those surveys (Fig. S1B),
173 although it underpredicted infections among individuals aged 40-60 years.

174 Calibration of the parameter that scaled the magnitude of SARS-CoV-2 importations [55, 56]
175 in our model resulted in a median of 1.118 (95% PPI: 0.654-1.456) imported infections per day
176 from February 1 to August 10. To ensure that the model reliably reproduced the high occurrence
177 of deaths observed in long-term care facilities, we seeded infections into those facilities at a daily
178 rate proportional to the prevalence of infection on that day; this calibrated proportion was 0.046
179 (95% PPI: 0.007-0.093). On the opposite end of the age spectrum, our calibration resulted in
180 a median estimate of susceptibility among children of 0.357 (95% CrI: 0.263-0.526), compared
181 to 0.788 (95% CrI: 0.651-0.946) in adults (Fig. S2). Our calibration resulted in an estimate of
182 transmissibility (median: 0.641; 95% CrI: 0.546-0.965) that corresponded to values of $R(t)$ during
183 the initial phase of the epidemic in Indiana of 1.67 (95% CrI: 0.47-3.57), which represents an
184 average of daily values across the month of February (Fig. 1A). Driven by a calibrated estimate

185 that the proportion of people sheltering in place rose in early March and peaked at a median of

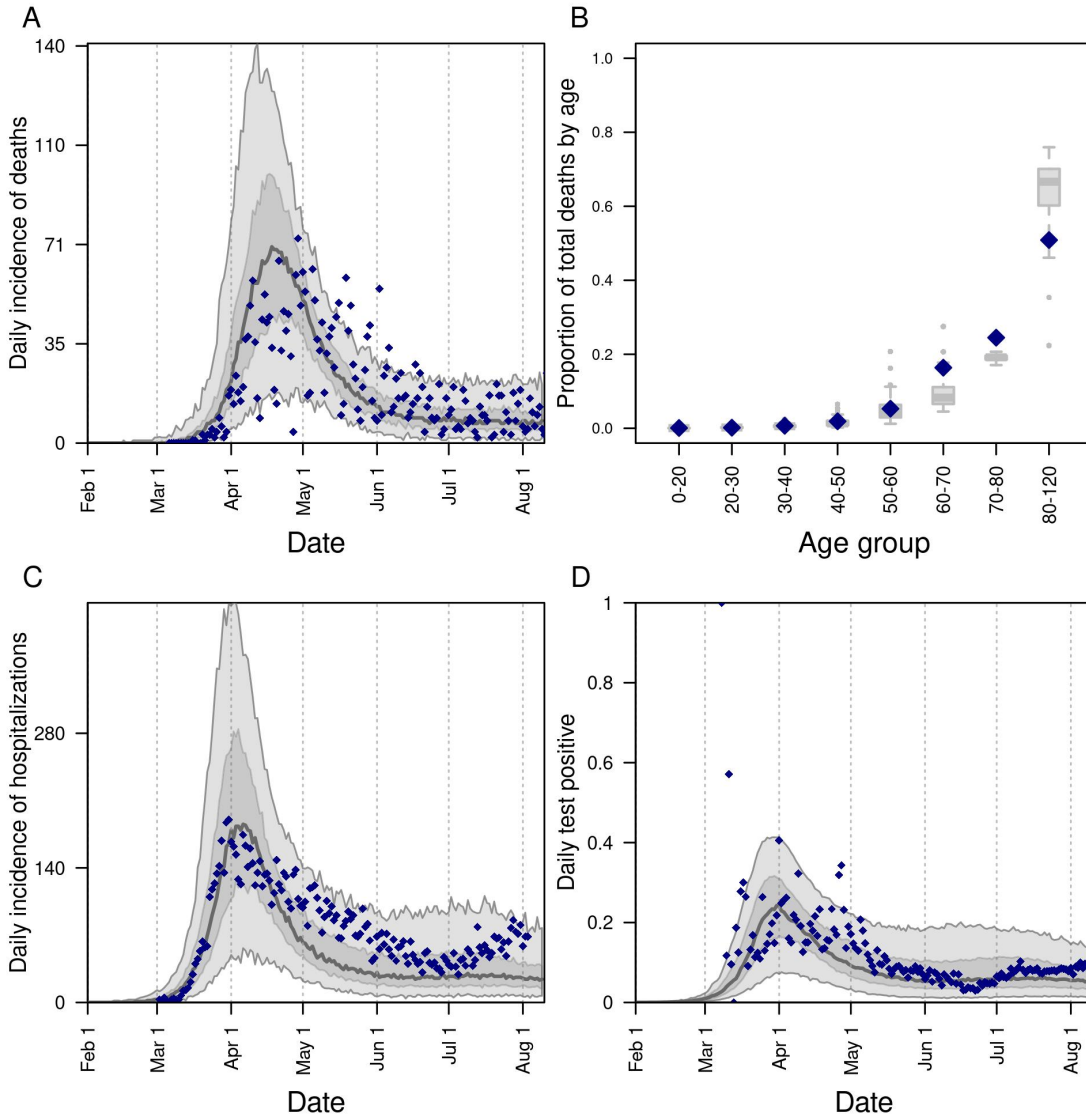


Figure 1. Model calibration to data: A) daily incidence of death; B) proportion of deaths through July 13 in decadal age bins; C) daily incidence of hospitalization; and D) daily proportion of tests administered that are positive for SARS-CoV-2. In all panels, blue diamonds represent data. In A, C, and D, the gray line is the median, the dark shaded region the 50% posterior predictive interval, and the light shaded region the 95% posterior predictive interval.

186 38.2% (95% CrI: 25.2-68.7%) on April 7 (Fig. S3A), our estimates of $R(t)$ dropped to a low of
187 0.57 (95% CrI: 0.41-0.75) on April 7 and have remained below 1 since (Fig. 1A). Also impacting
188 our estimates of $R(t)$ is the increasing use of face masks in the community, which we estimated
189 at 0.50 (95% CrI: 0.458-0.545) as of July 19 (Fig. S3B). Note that this estimated distribution
190 of community face-mask adherence does not differ between scenarios and is not the same as the
191 level of adherence in schools, which we imposed at different levels depending on the scenario.

192 In the event that schools reopen at full capacity and without any use of face masks, our model
193 projects that $R(t)$ would increase to 1.94 (95% CrI: 1.47-2.20) by mid-September (Fig. 2A). This
194 assumes that levels of sheltering in place and face-mask adherence in the community remain at
195 their estimated levels as of August 13 (Fig. S3B). Consistent with our model's prediction that
196 schools contributed appreciably to transmission early in the epidemic (median: 24.6%; 95% CrI:
197 23.2-27.7%), this increase in transmission is associated with an increase in the proportion of
198 infections arising in schools upon their reopening (Fig. 2B). The sensitivity of the proportion
199 of infections arising in schools to model parameters was highest for the inflection point of the
200 age-susceptibility relationship, the transmissibility parameter, and the rate at which infections
201 were imported into long-term care facilities (Fig. S7). This increase in infections arising in
202 schools is projected to give rise to additional transmission statewide (Fig. 2C). An example of
203 transmission chains arising from schools and spilling out into school-affiliated families and the
204 broader community is shown in Fig. 3.

205 In the event that schools remain open throughout the semester and no other policies or
206 behavioral responses occur, the increase in $R(t)$ driven by reopening schools at full capacity and
207 without the use of face masks would be projected to result in 2.49 million (95% CrI: 2.08-2.70
208 million) infections (Fig. 4A) and 9,117 (95% CrI: 6,117-6,248) deaths (Fig. 4B) from Indiana's
209 population as a whole between August 24 and December 31. At the other extreme, if schools
210 were to go to remote instruction and all children remained at home, our model projects that $R(t)$
211 would remain near current levels through the remainder of 2020 (Fig. S4A). Again, this assumes
212 that levels of sheltering in place and face-mask adherence in the community as a whole remain at
213 their estimated levels as of August 13. Under this scenario, transmission would continue through
214 contacts at workplaces, within homes, and elsewhere in the community (Fig. S4B), with 19,527
215 (95% CrI: 4,651-56,502) infections (Fig. S4C) and 360 (95% CrI: 67-967) deaths between August
216 24 and December 31.

217 Differing policies on the capacity at which schools operate in person and enforce the use of
218 face masks have a strong influence on the projected statewide burden of COVID-19. If schools
219 operate at 50% capacity and achieve high face-mask adherence, the number of infections and
220 deaths that we project is similar to what we project under the scenario in which schools operate
221 remotely (Fig. 4, Table S1). Of these two policies, projections of infections and deaths were more
222 sensitive to the capacity at which schools operate, with the worst outcomes projected to occur
223 when schools operate at full capacity and with low face-mask adherence. Under this scenario,
224 cumulative infections statewide were projected to be 300% (95% CrI: 280-310%) greater than if
225 schools operated remotely, and cumulative deaths statewide were projected to be 50% (95% CrI:
226 50-60%) greater (Table S1). The sensitivity of these results to model parameters was relatively
227 high for parameters that define the age-susceptibility relationship and, in some cases, for the

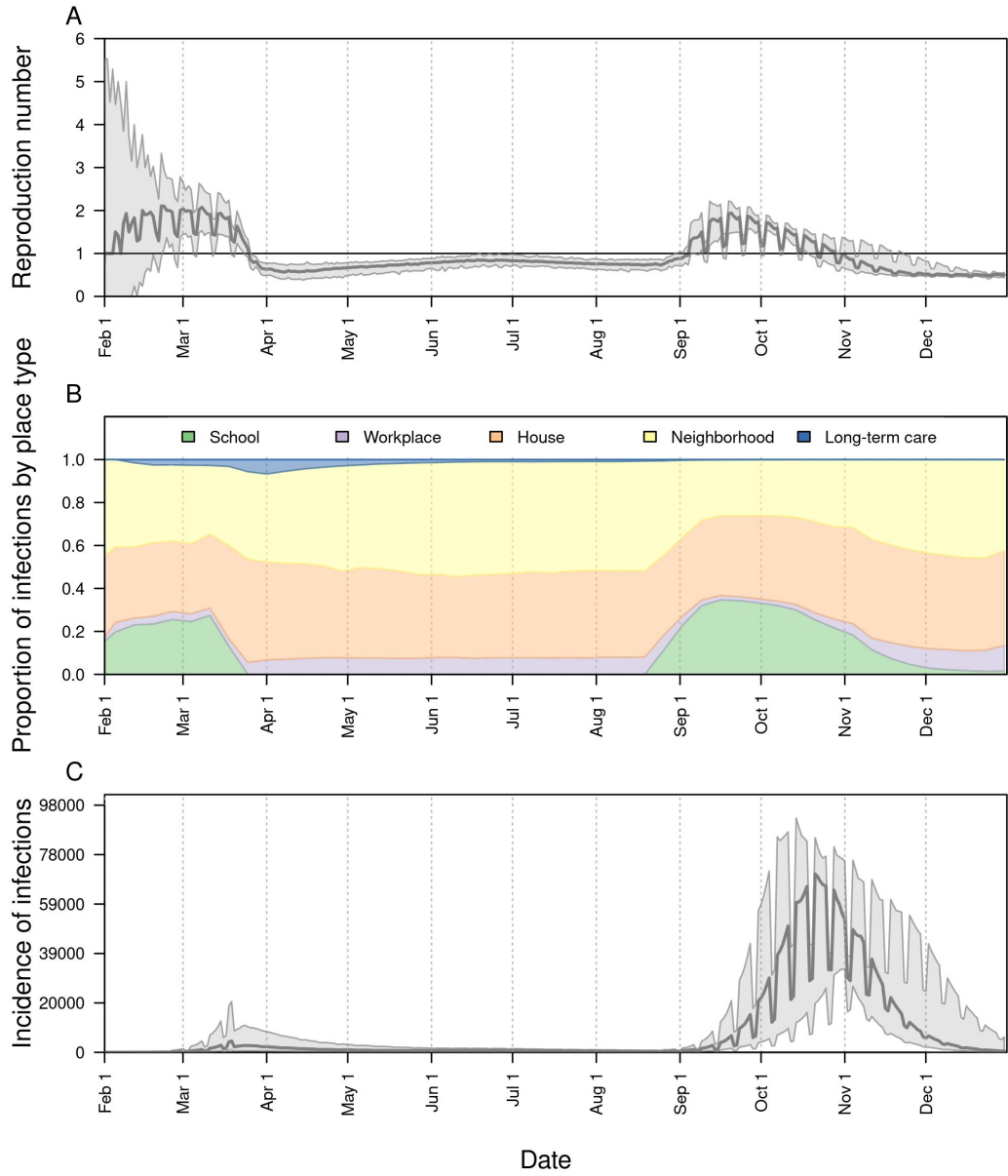


Figure 2. The impact of school reopening in Indiana on: A) the reproduction number, $R(t)$, over time; B) the proportion of infections acquired in different location types over time; and C) the daily incidence of infection over time. In all panels, schools reopened on August 24. In A and C, the line represents the median, and the shaded region represents the 50% posterior predictive interval.

228 transmissibility and shelter-in-place compliance parameters (Fig. S6).

229 The burden of COVID-19 associated with reopening schools differed for students, teachers,
230 and their families. Relative to a scenario with remote instruction, risk of infection and symp-
231 tomatic infection was greatest for students (Fig. 5, left column), with a hundred-fold or greater
232 increase in the risk of infection if schools operate at full capacity with moderate or low face-mask
233 adherence (Table S2). Due to their older ages, teachers and families experienced a much higher
234 risk of death under scenarios with high capacity and moderate or low face-mask adherence, as
235 compared with a scenario with remote instruction (Fig. 5, center & right columns). Under a
236 scenario with high capacity and low face-mask adherence, there was a 227-fold higher risk of
237 death for teachers (Table S3) and a 266-fold higher risk of death for family members (Table S4).
238 At the same time, the risk of death under a scenario with high capacity and low face-mask
239 adherence was around half the risk of death if schools were to operate at full capacity with no
240 masks (Tables S7 & S8).

241 4 Discussion

242 Our model provides a detailed, demographically realistic representation of SARS-CoV-2 trans-
243 mission in Indiana that is consistent both with data to which it was calibrated and to data that
244 was withheld from calibration. In contrast to models that rely on assumptions about intervention

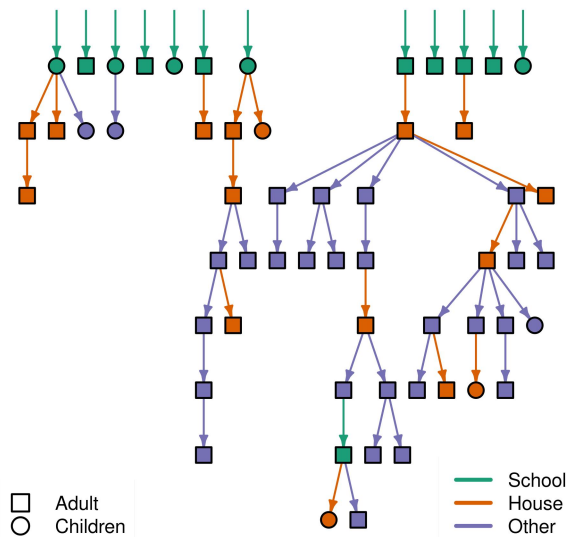


Figure 3. Example transmission tree of SARS-CoV-2 from one simulation of the model for Saint Joseph County, Indiana. Green shapes at the top represent agents in the model infected at school, and arrows descending from them and other shapes show transmission events in school-affiliated households (orange) and the community at large (purple) that trace back to infections originally acquired in schools. Different shapes distinguish children (circles) from adults (squares).

245 impacts or estimate them statistically [2, 57], our model makes predictions about intervention
246 impacts based on first-principles assumptions about individual-level behavior and contact pat-
247 terns. Consistent with results from other analyses [2, 57, 20], the inputs and assumptions in
248 our model led to a prediction that schools made a considerable contribution to SARS-CoV-2
249 transmission in February and early March, prior to large-scale changes in behavior. Extending
250 that, a primary result of our analysis is that schools could, once again, make a considerable
251 contribution to SARS-CoV-2 transmission if they resume normal activity in the fall semester.

252 Our results indicate that operating at reduced capacity and achieving high face-mask adher-
253 ence would reduce the burden of COVID-19 in schools and across the state. In the event that
254 both interventions are pursued fully, our model projects that infections and deaths statewide
255 would be around 10% greater than under a scenario with fully remote instruction. In the event
256 that schools operate at full capacity, our model projects that infections and deaths statewide
257 could be one to two orders of magnitude greater than under a scenario with fully remote instruc-
258 tion, especially if there is poor face-mask adherence in schools. The impacts associated with
259 reducing capacity result from reductions in both the number of contacts within the school and
260 the probability that an infected student would be in attendance in the first place, similar to the
261 logic behind why smaller gatherings are associated with reduced risk of transmission [3, 58, 59].

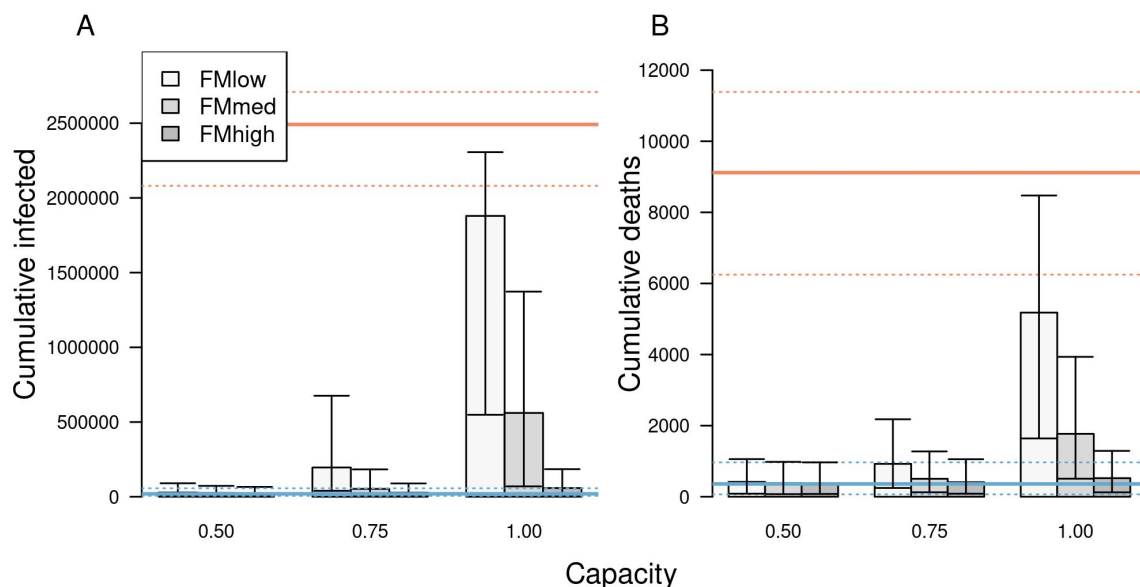


Figure 4. The impact of different school reopening strategies on A) cumulative infections and B) cumulative deaths in Indiana between August 24 and December 31. Scenarios are defined by the capacity at which schools operate (x-axis) and face-mask adherence (shading). Orange lines represent projections under a scenario of school reopening at full capacity without masks (solid: median; dotted: 95% posterior predictive interval). Blue lines represent a scenario where schools operate remotely. Error bars indicate inter-quartile ranges.

262 Although the scenarios we considered resulted in projected impacts spanning nearly the full
263 range between fully remote instruction and fully in-person instruction with no face masks, they
264 are a simplification of the full range of scenarios of how schools could operate this fall. Scenarios
265 that we did not explore include different groups of students attending in person or remotely [60],
266 varying degrees of modularization within schools [61], and the implementation of testing-based
267 control strategies in schools [62]. A related simplification of our statewide analysis is that the
268 state will, in reality, consist of a patchwork of policies across districts. In light of this complexity
269 that our model does not capture, our results should be interpreted with caution in setting specific,
270 quantitative targets for capacity or face-mask adherence. For any scenario though, our results
271 illustrate the importance of reducing capacity and maximizing face-mask adherence to the extent
272 possible, as do other modeling studies [60, 61, 62, 63, 64].

273 The burden of COVID-19 associated with reopening schools is not expected to fall evenly
274 across the state's population. Under scenarios with schools operating at full capacity, our model
275 projects that hundreds of thousands of children could be infected during the fall semester.
276 Whereas very few deaths are expected among infected children, the numbers of deaths among
277 teachers and school-affiliated families could number in the hundreds. In comparison, the total
278 number of deaths projected across the state is projected to be in the low thousands, meaning
279 that adults with close ties to schools could represent a sizable fraction of deaths across the state
280 in coming months, if schools operate at full capacity and with low face-mask adherence. Im-
281 portantly, the magnitude of these projections depend further on factors outside the control of
282 schools [2]. In the absence of school reopening, our projections assume steady, controlled levels
283 of transmission with $R(t) < 1$. Changes in government policies, individual behavior, and face-
284 mask adherence in the community all have the potential to alter this trajectory for the state as
285 a whole, as well as its schools [2, 31, 65].

286 A critical assumption of our analysis is that children are capable of being infected with SARS-
287 CoV-2 and transmitting it to others at meaningful levels. Although the burden of severe disease
288 skews strongly towards older ages [22, 66, 8], there are other lines of evidence that support
289 our assumption. These include a contact-tracing study that found no distinguishable difference
290 between infectivity of children and adults [26], several studies that found no distinguishable
291 difference in viral load between children and adults [67, 37, 36, 68], a study that observed a
292 greater secondary attack rate among children in homes [26], and a modeling study that found
293 no evidence that children were less infectious [69]. More direct evidence comes from COVID-19
294 outbreaks that have already been observed in schools, including one in a high school in Israel
295 in which 13.2% of students and 16.6% of staff were infected in just 10 days [70]. Even more
296 pertinent, some schools in Indiana recently reopened and have already reported cases of COVID-
297 19 among students [71]. Our analysis offers perspective on what those initial cases could give
298 rise to in coming months, depending on the degree to which schools choose to operate at reduced
299 capacity and enforce face-mask adherence.

300 There is now a growing body of evidence that school closures contributed to mitigating the
301 first wave of the epidemic and could lead to rising case numbers if relaxed [6, 62]. Our study
302 adds to this evidence, and suggests an even greater impact of school reopening than several
303 other studies [64, 62, 61, 72, 60]. This is due in part to our assumption that asymptomatic and

304 symptomatic infections contribute similarly to transmission [26, 67, 37, 36, 68], and in part to
305 our model's ability to capture chains of transmission within schools and extending out into the
306 community. Our study echoes several modeling studies in emphasizing the importance of reducing
307 school capacity to impede transmission [61, 62, 63, 64, 72]. Taking all this evidence together,
308 those deciding on strategies to safely reopen schools should strongly consider operating at reduced
309 capacity and strictly enforcing face-mask adherence. Both schools, and the communities in which
310 they are embedded, stand to be affected by these policy choices.

311 5 Acknowledgements

312 This work was supported by an NSF RAPID grant to TAP (DEB 2027718), an Arthur J. Schmitt
313 Fellowship and Eck Institute for Global Health Fellowship to RJO, and a Richard and Peggy
314 Notabaert Premier Fellowship to MP. We thank the University of Notre Dame Center for Research
315 Computing for computing resources.

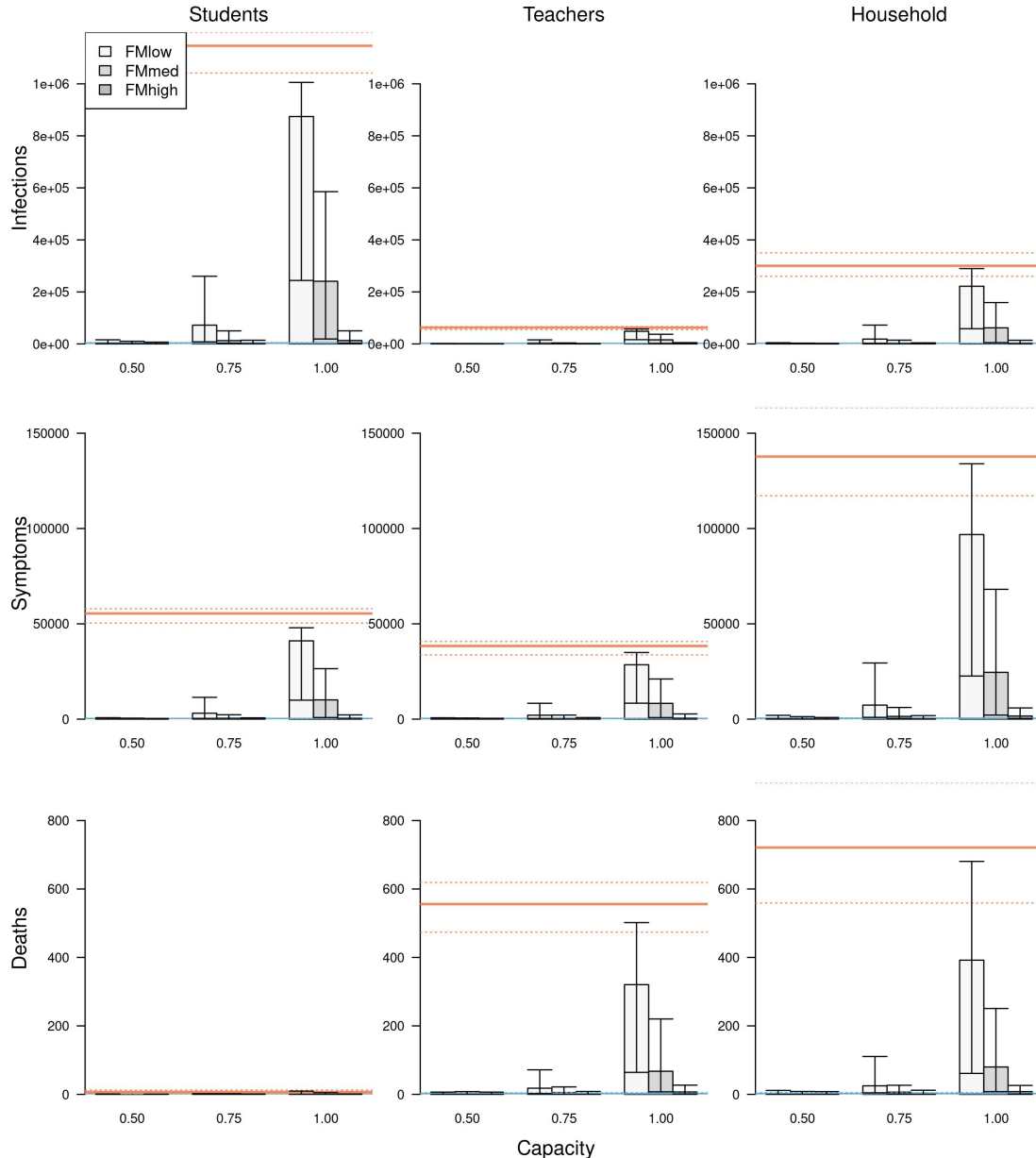


Figure 5. The impact of different school reopening strategies on cumulative infections (top row), cumulative symptomatic infections (middle row), and cumulative deaths (bottom row) in Indiana between August 24 and December 31. These outcomes are presented separately for students (left column), teachers (middle column), and school-affiliated families (right column). Scenarios are defined by the capacity at which schools operate (x-axis) and face-mask adherence (shading). Orange lines represent projections under a scenario of school reopening at full capacity without masks (solid: median; dotted: 95% posterior predictive interval). Blue lines represent a scenario where schools operate remotely. Error bars indicate inter-quartile ranges.

316 References

- 317 [1] The New York Times. "Coronavirus in the U.S.: Latest Map and Case Count". en-US. In:
318 *The New York Times* (July 2020). ISSN: 0362-4331.
- 319 [2] H Juliette T Unwin et al. "State-Level Tracking of COVID-19 in the United States". In:
320 *medRxiv* (2020). DOI: 10.1101/2020.07.13.20152355. eprint: <https://www.medrxiv.org/content/early/2020/07/14/2020.07.13.20152355.full.pdf>.
- 321 [3] Seth Flaxman et al. "Estimating the Effects of Non-Pharmaceutical Interventions on COVID-
322 19 in Europe". In: *Nature* 584.7820 (Aug. 2020), pp. 257–261. ISSN: 1476-4687. DOI: 10.
323 1038/s41586-020-2405-7.
- 324 [4] *Coronavirus Government Response Tracker*. en. <https://www.bsg.ox.ac.uk/research/research-projects/coronavirus-government-response-tracker>.
- 325 [5] Hamada S Badr et al. "Association between Mobility Patterns and COVID-19 Transmission
326 in the USA: A Mathematical Modelling Study". In: *The Lancet Infectious Diseases* (2020).
327 ISSN: 1473-3099. DOI: 10.1016/S1473-3099(20)30553-3.
- 328 [6] Katherine A. Auger et al. "Association between Statewide School Closure and COVID-19
329 Incidence and Mortality in the US". In: *JAMA* (July 2020). ISSN: 0098-7484. DOI: 10.1001/
330 *jama*.2020.14348.
- 331 [7] Charles Courtemanche et al. "Strong Social Distancing Measures In The United States
332 Reduced The COVID-19 Growth Rate: Study Evaluates the Impact of Social Distancing
333 Measures on the Growth Rate of Confirmed COVID-19 Cases across the United States." In:
334 *Health Affairs* (2020), pp. 10–1377.
- 335 [8] *ISDH - Novel Coronavirus: Indiana COVID-19 Dashboard*. <https://www.coronavirus.in.gov/2393.htm>.
- 336 [9] Kenne A. Dibner, Heidi A. Schweingruber, and Dimitri A. Christakis. "Reopening K-12
337 Schools during the COVID-19 Pandemic: A Report from the National Academies of Sciences,
338 Engineering, and Medicine". In: *JAMA* (July 2020). ISSN: 0098-7484. DOI: 10.1001/
339 *jama*.2020.14745.
- 340 [10] *President Donald J. Trump Is Supporting America's Students and Families By Encouraging
341 the Safe Reopening of America's Schools*. en-US. <https://www.whitehouse.gov/briefings-statements/president-donald-j-trump-supporting-americas-students-families-encouraging-safe-reopening-americas-schools/>.
- 342 [11] Indiana State Department of Health, Indiana Department of Education, and Indiana Family
343 and Social Services Administration. *IN-CLASS: Indiana's Considerations for Learning
344 and Safe Schools. COVID-19 Health and Safety Re-Entry Guidance*. June 2020.
- 345 [12] Charlotte Jackson et al. "School Closures and Influenza: Systematic Review of Epidemiological
346 Studies". In: *BMJ Open* 3.2 (2013). ISSN: 2044-6055. DOI: 10.1136/bmjopen-2012-
347 002149. eprint: <https://bmjopen.bmjjournals.com/content/3/2/e002149.full.pdf>.
- 348
- 349
- 350
- 351

- 352 [13] Shoko Kawano and Masayuki Kakehashi. "Substantial Impact of School Closure on the
353 Transmission Dynamics during the Pandemic Flu H1N1-2009 in Oita, Japan". In: *PLOS*
354 *ONE* 10.12 (Dec. 2015), pp. 1–15. DOI: 10.1371/journal.pone.0144839.
- 355 [14] Simon Cauchemez et al. "Closure of Schools during an Influenza Pandemic". In: *The*
356 *Lancet Infectious Diseases* 9.8 (2009), pp. 473–481. ISSN: 1473-3099. DOI: 10.1016/S1473-
357 3099(09)70176-8.
- 358 [15] Niel Hens et al. "Estimating the Impact of School Closure on Social Mixing Behaviour
359 and the Transmission of Close Contact Infections in Eight European Countries". In: *BMC*
360 *infectious diseases* 9.1 (2009), p. 187.
- 361 [16] Simon Cauchemez et al. "Estimating the Impact of School Closure on Influenza Transmis-
362 sion from Sentinel Data". In: *Nature* 452.7188 (Apr. 2008), pp. 750–754. ISSN: 1476-4687.
363 DOI: 10.1038/nature06732.
- 364 [17] Charlotte Jackson et al. "The Effects of School Closures on Influenza Outbreaks and Pan-
365 demics: Systematic Review of Simulation Studies". In: *PLOS ONE* 9.5 (May 2014), pp. 1–
366 10. DOI: 10.1371/journal.pone.0097297.
- 367 [18] Sten H Vermund and Virginia E Pitzer. "Asymptomatic Transmission and the Infection
368 Fatality Risk for COVID-19: Implications for School Reopening". In: *Clinical Infectious*
369 *Diseases* (June 2020). ISSN: 1058-4838. DOI: 10.1093/cid/ciaa855.
- 370 [19] Nicholas G. Davies et al. "Age-Dependent Effects in the Transmission and Control of
371 COVID-19 Epidemics". In: *Nature Medicine* (June 2020). ISSN: 1546-170X. DOI: 10.1038/
372 s41591-020-0962-9.
- 373 [20] Juanjuan Zhang et al. "Changes in Contact Patterns Shape the Dynamics of the COVID-
374 19 Outbreak in China". In: *Science* 368.6498 (2020), pp. 1481–1486. ISSN: 0036-8075. DOI:
375 10.1126/science.abb8001. eprint: <https://science.sciencemag.org/content/368/6498/1481.full.pdf>.
- 377 [21] Joseph T Wu et al. "Estimating Clinical Severity of COVID-19 from the Transmission
378 Dynamics in Wuhan, China". In: *Nature medicine* (2020), pp. 1–5.
- 379 [22] Robert Verity et al. "Estimates of the Severity of Coronavirus Disease 2019: A Model-
380 Based Analysis". eng. In: *The Lancet. Infectious Diseases* (Mar. 2020). ISSN: 1474-4457.
381 DOI: 10.1016/S1473-3099(20)30243-7.
- 382 [23] Willem et al. "The Impact of Contact Tracing and Household Bubbles on Deconfinement
383 Strategies for COVID-19: An Individual-Based Modelling Study". In: *medRxiv* (2020). DOI:
384 10.1101/2020.07.01.20144444. eprint: <https://www.medrxiv.org/content/early/2020/07/06/2020.07.01.20144444.full.pdf>.
- 386 [24] Christine M Szablewski. "SARS-CoV-2 Transmission and Infection among Attendees of an
387 Overnight Camp—Georgia, June 2020". In: *MMWR. Morbidity and mortality weekly report*
388 69 (2020), pp. 1023–1025. DOI: <http://dx.doi.org/10.15585/mmwr.mm6931e1>.

- 389 [25] Young Joon Park et al. "Contact Tracing during Coronavirus Disease Outbreak, South
390 Korea, 2020". In: *Emerging Infectious Disease journal* 26.10 (2020). ISSN: 1080-6059. DOI:
391 10.3201/eid2610.201315.
- 392 [26] Pirous Fateh-Moghadam et al. "Contact Tracing during Phase I of the COVID-19 Pandemic
393 in the Province of Trento, Italy: Key Findings and Recommendations". In: *medRxiv* (2020).
394 DOI: 10.1101/2020.07.16.20127357. eprint: <https://www.medrxiv.org/content/early/2020/07/29/2020.07.16.20127357.full.pdf>.
- 396 [27] George Psacharopoulos et al. "Lost Wages: The COVID-19 Cost of School Closures". In:
397 *World Bank Policy Research Working Paper* 9246 (2020).
- 398 [28] Danielle G. Dooley, Asad Bandealy, and Megan M. Tschudy. "Low-Income Children and
399 Coronavirus Disease 2019 (COVID-19) in the US". In: *JAMA Pediatrics* (May 2020). ISSN:
400 2168-6203. DOI: 10.1001/jamapediatrics.2020.2065. eprint: https://jamanetwork.com/journals/jamapediatrics/articlepdf/2766115/jamapediatrics\textbackslash_doleyley\textbackslash_2020\textbackslash_vp\textbackslash_200021.pdf.
- 403 [29] Wim Van Lancker and Zachary Parolin. "COVID-19, School Closures, and Child Poverty:
404 A Social Crisis in the Making". In: *The Lancet Public Health* 5.5 (2020), e243–e244.
- 405 [30] John J Grefenstette et al. "FRED (A Framework for Reconstructing Epidemic Dynamics):
406 An Open-Source Software System for Modeling Infectious Diseases and Control Strategies
407 Using Census-Based Populations". In: *BMC public health* 13.1 (2013), p. 940.
- 408 [31] Derek K Chu et al. "Physical Distancing, Face Masks, and Eye Protection to Prevent
409 Person-to-Person Transmission of SARS-CoV-2 and COVID-19: A Systematic Review and
410 Meta-Analysis". In: *The Lancet* (2020).
- 411 [32] W D Wheaton. "2005-2009 U.S. Synthetic Population Ver.2. RTI International". In: (2012).
- 412 [33] Joël Mossong et al. "Social Contacts and Mixing Patterns Relevant to the Spread of In-
413 fectious Diseases". In: *PLOS Medicine* 5.3 (Mar. 2008), pp. 1–1. DOI: 10.1371/journal.pmed.0050074.
- 415 [34] Tapiwa Ganyani et al. "Estimating the Generation Interval for COVID-19 Based on Sym-
416 tom Onset Data". en. In: *medRxiv* (Mar. 2020), p. 2020.03.05.20031815. ISSN: 10.1101/2020.03.05.20031815.
417 DOI: 10.1101/2020.03.05.20031815.
- 418 [35] Kenji Mizumoto et al. "Estimating the Asymptomatic Proportion of Coronavirus Disease
419 2019 (COVID-19) Cases on Board the Diamond Princess Cruise Ship, Yokohama, Japan,
420 2020". en. In: *Eurosurveillance* 25.10 (Mar. 2020), p. 2000180. ISSN: 1560-7917. DOI: 10.2807/1560-7917.ES.2020.25.10.2000180.
- 422 [36] Lael M. Yonker et al. "Pediatric SARS-CoV-2: Clinical Presentation, Infectivity, and Im-
423 mune Responses". In: *The Journal of Pediatrics* (). ISSN: 0022-3476. DOI: 10.1016/j.jpeds.2020.08.037.

- 425 [37] Taylor Heald-Sargent et al. "Age-Related Differences in Nasopharyngeal Severe Acute Res-
426piratory Syndrome Coronavirus 2 (SARS-CoV-2) Levels in Patients with Mild to Moderate
427Coronavirus Disease 2019 (COVID-19)". In: *JAMA Pediatrics* (July 2020). ISSN: 2168-
4286203. DOI: 10.1001/jamapediatrics.2020.3651. eprint: https://jamanetwork.com/journals/jamapediatrics/articlepdf/2768952/jamapediatrics/textbackslash/healdsargent/textbackslash/_2020/textbackslash_1d/textbackslash_200036.pdf.
- 431
- 432 [38] Shixiong Hu et al. "Infectivity, Susceptibility, and Risk Factors Associated with SARS-CoV-
4332 Transmission under Intensive Contact Tracing in Hunan, China". In: *medRxiv* (2020).
434DOI: 10.1101/2020.07.23.20160317. eprint: <https://www.medrxiv.org/content/early/2020/08/07/2020.07.23.20160317.full.pdf>.
- 435
- 436 [39] Stephen A. Lauer et al. "The Incubation Period of Coronavirus Disease 2019 (COVID-19)
437From Publicly Reported Confirmed Cases: Estimation and Application". en. In: *Annals of
438Internal Medicine* (Mar. 2020). ISSN: 0003-4819. DOI: 10.7326/M20-0504.
- 439
- 440 [40] Qifang Bi et al. "Epidemiology and Transmission of COVID-19 in 391 Cases and 1286 of
441Their Close Contacts in Shenzhen, China: A Retrospective Cohort Study". In: *The Lancet
Infectious Diseases* (2020).
- 442
- 443 [41] The Novel Coronavirus Pneumonia Emergency Response Epidemiology Team. "The Epi-
444demiological Characteristics of an Outbreak of 2019 Novel Coronavirus Diseases (COVID-
44519) — China, 2020". en. In: *China CDC Weekly* 2.8 (Feb. 2020), pp. 113–122. ISSN: 2096-
7071.
- 446
- 447 [42] T Alex Perkins et al. "Calling in Sick: Impacts of Fever on Intra-Urban Human Mobility".
448 In: *Proceedings of the Royal Society of London B: Biological Sciences* 283.1834 (2016). ISSN:
0962-8452. DOI: 10.1098/rspb.2016.0390.
- 449
- 450 [43] Team CDC COVID et al. "Characteristics of Health Care Personnel with COVID-19—United
451States, February 12–April 9, 2020." In: *MMWR. Morbidity and Mortality Weekly Report*
(2020).
- 452
- 453 [44] IHME COVID-19 health service utilization forecasting Team and Christopher JL Murray.
454 "Forecasting COVID-19 Impact on Hospital Bed-Days, ICU-Days, Ventilator-Days and
455Deaths by US State in the next 4 Months". en. In: *medRxiv* (Mar. 2020), p. 2020.03.27.20043752.
DOI: 10.1101/2020.03.27.20043752.
- 456
- 457 [45] *COVID-19 Community Mobility Report*. <https://www.google.com/covid19/mobility?hl=en>.
- 458
- 459 [46] Christopher J Cronin and William N Evans. *Private Precaution and Public Restrictions:
What Drives Social Distancing and Industry Foot Traffic in the COVID-19 Era?* Working
Paper 27531. National Bureau of Economic Research, July 2020. DOI: 10.3386/w27531.
- 460
- 461 [47] *Google Trends*. en-US. <https://trends.google.com/trends/?geo=US>.
- 462 [48] New York Times and Dynata. *Estimates from The New York Times, Based on Roughly
250,000 Interviews Conducted by Dynata from July 2 to July 14*. Tech. rep.

- 463 [49] The COVID Tracking Project. *Michigan*. en. <https://covidtracking.com/data/state/michigan>.
464 2020.
- 465 [50] Aaron A. King et al. *pomp: Statistical Inference for Partially Observed Markov Processes*.
466 Manual. 2020.
- 467 [51] Aaron A. King, Dao Nguyen, and Edward L. Ionides. “Statistical Inference for Partially
468 Observed Markov Processes via the R Package pomp”. In: *Journal of Statistical Software*
469 69.12 (2016), pp. 1–43. DOI: 10.18637/jss.v069.i12.
- 470 [52] Nir Menachemi et al. “Population Point Prevalence of SARS-CoV-2 Infection Based on
471 a Statewide Random Sample—Indiana, April 25–29, 2020”. In: *Morbidity and Mortality
472 Weekly Report* 69.29 (2020), p. 960.
- 473 [53] Andrea Zeek. *COVID-19 Study’s Phase 2 Results Show Spread of Virus in Indiana*. en.
474 <https://news.iu.edu/stories/2020/06/iupui/releases/17-fairbanks-isdh-second-phase-covid-19-testing-indiana-research.html>. June 2020.
- 475 [54] Mark Stevenson with contributions from Telmo Nunes et al. *epiR: Tools for the Analysis
476 of Epidemiological Data*. Manual. 2020.
- 477 [55] T. Alex Perkins et al. “Estimating Unobserved SARS-CoV-2 Infections in the United
478 States”. In: *Proceedings of the National Academy of Sciences* (2020). ISSN: 0027-8424. DOI:
479 10.1073/pnas.2005476117. eprint: <https://www.pnas.org/content/early/2020/08/20/2005476117.full.pdf>.
- 480 [56] *MIDAS Network, Midas-Network/COVID-19*. GitHub. <https://github.com/midas-net-work/COVID-19>.
- 481 [57] Susanna Esposito and Nicola Principi. “School Closure during the Coronavirus Disease
482 2019 (COVID-19) Pandemic: An Effective Intervention at the Global Level?” In: *JAMA
483 Pediatrics* (May 2020). ISSN: 2168-6203. DOI: 10.1001/jamapediatrics.2020.1892.
484 eprint: https://jamanetwork.com/journals/jamapediatrics/articlepdf/2766114/jamapediatrics\textbackslash_esposito\textbackslash_2020\textbackslash_vp\textbackslash_200019.pdf.
- 485 [58] Nor Fazila Che Mat et al. “A Single Mass Gathering Resulted in Massive Transmission
486 of COVID-19 Infections in Malaysia with Further International Spread”. In: *Journal of
487 Travel Medicine* 27.3 (Apr. 2020). ISSN: 1708-8305. DOI: 10.1093/jtm/taaa059. eprint:
488 <https://academic.oup.com/jtm/article-pdf/27/3/taaa059/33226391/taaa059.pdf>.
- 489 [59] Sukbin Jang, Si Hyun Han, and Ji-Young Rhee. “Cluster of Coronavirus Disease Associated
490 with Fitness Dance Classes, South Korea”. eng. In: *Emerging infectious diseases* 26.8 (Aug.
491 2020), pp. 1917–1920. ISSN: 1080-6059. DOI: 10.3201/eid2608.200633.
- 492 [60] Matt J Keeling et al. “The Impact of School Reopening on the Spread of COVID-19 in
493 England”. In: *medRxiv* (2020). DOI: 10.1101/2020.06.04.20121434. eprint: <https://www.medrxiv.org/content/early/2020/06/05/2020.06.04.20121434.full.pdf>.

- 500 [61] Jennifer R Head et al. "The Effect of School Closures and Reopening Strategies on COVID-
501 19 Infection Dynamics in the San Francisco Bay Area: A Cross-Sectional Survey and Mod-
502 eling Analysis". In: *medRxiv* (2020). DOI: 10.1101/2020.08.06.20169797. eprint: <https://www.medrxiv.org/content/early/2020/08/07/2020.08.06.20169797.full.pdf>.
- 504 [62] Jasmina Panovska-Griffiths et al. "Determining the Optimal Strategy for Reopening Schools,
505 the Impact of Test and Trace Interventions, and the Risk of Occurrence of a Second COVID-
506 19 Epidemic Wave in the UK: A Modelling Study". In: *The Lancet Child & Adolescent
507 Health* (2020). ISSN: 2352-4642. DOI: 10.1016/S2352-4642(20)30250-9.
- 508 [63] Benjamin Lee et al. "Modeling the Impact of School Reopening on SARS-CoV-2 Trans-
509 mission". In: *Research Square* (2020).
- 510 [64] Alfonso Landeros et al. "An Examination of School Reopening Strategies during the SARS-
511 CoV-2 Pandemic". In: *medRxiv* (2020). DOI: 10.1101/2020.08.05.20169086. eprint:
512 <https://www.medrxiv.org/content/early/2020/08/06/2020.08.05.20169086.full.pdf>.
- 514 [65] Richard OJH Stutt et al. "A Modelling Framework to Assess the Likely Effectiveness of
515 Facemasks in Combination with 'Lock-down' in Managing the COVID-19 Pandemic". In:
516 *Proceedings of the Royal Society A* 476.2238 (2020), p. 20200376.
- 517 [66] *COVID-19 Hospitalizations*. https://gis.cdc.gov/grasp/COVIDNet/COVID19_3.html.
- 518 [67] Enrico Lavezzo et al. "Suppression of a SARS-CoV-2 Outbreak in the Italian Municipality
519 of Vo". In: *Nature* 584.7821 (Aug. 2020), pp. 425–429. ISSN: 1476-4687. DOI: 10.1038/
520 s41586-020-2488-1.
- 521 [68] Terry C Jones et al. "An Analysis of SARS-CoV-2 Viral Load by Patient Age". In: *medRxiv*
522 (2020). DOI: 10.1101/2020.06.08.20125484. eprint: <https://www.medrxiv.org/content/early/2020/06/09/2020.06.08.20125484.full.pdf>.
- 524 [69] Itai Dattner et al. "The Role of Children in the Spread of COVID-19: Using Household
525 Data from Bnei Brak, Israel, to Estimate the Relative Susceptibility and Infectivity of
526 Children". In: *medRxiv* (2020). DOI: 10.1101/2020.06.03.20121145. eprint: <https://www.medrxiv.org/content/early/2020/06/05/2020.06.03.20121145.full.pdf>.
- 528 [70] Chen Stein-Zamir et al. "A Large COVID-19 Outbreak in a High School 10 Days after
529 Schools' Reopening, Israel, May 2020". In: *Eurosurveillance* 25.29 (2020), p. 2001352. DOI:
530 10.2807/1560-7917.ES.2020.25.29.2001352.
- 531 [71] Hannah Reed. "Some school districts in Northwest Indiana are reporting COVID-19 cases
532 and quarantined students". English (United States), en-US. In: *Chicago Tribune* ().
- 533 [72] Elaheh Abdollahi et al. "Simulating the Effect of School Closure during COVID-19 Out-
534 breaks in Ontario, Canada". In: *BMC Medicine* 18.1 (July 2020), p. 230. ISSN: 1741-7015.
535 DOI: 10.1186/s12916-020-01705-8.

536 Supplementary material

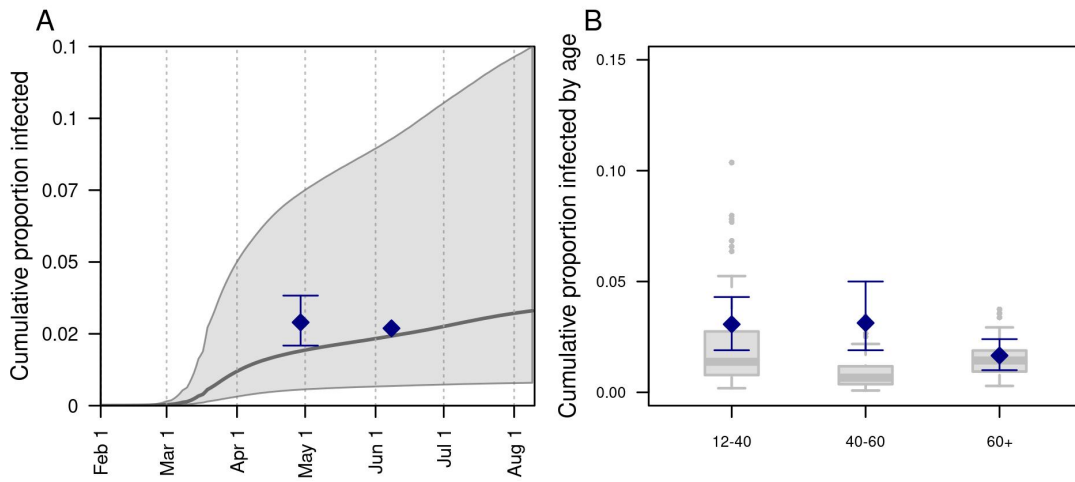


Figure S1. Model comparison with data withheld from fitting. We validated the model's predictions against data withheld from fitting on A) the cumulative proportion of the population of Indiana infected through late April and early June, and B) the cumulative proportion infected among individuals aged 12-40, 40-60, and 60+. Data are shown in navy and come from a random, statewide serological survey [52]. Model predictions are shown in gray. In A, the line and band indicate the median and 95% posterior predictive interval. In B, lines, boxes, and error bars indicate median, interquartile range, and 95% posterior predictive interval.

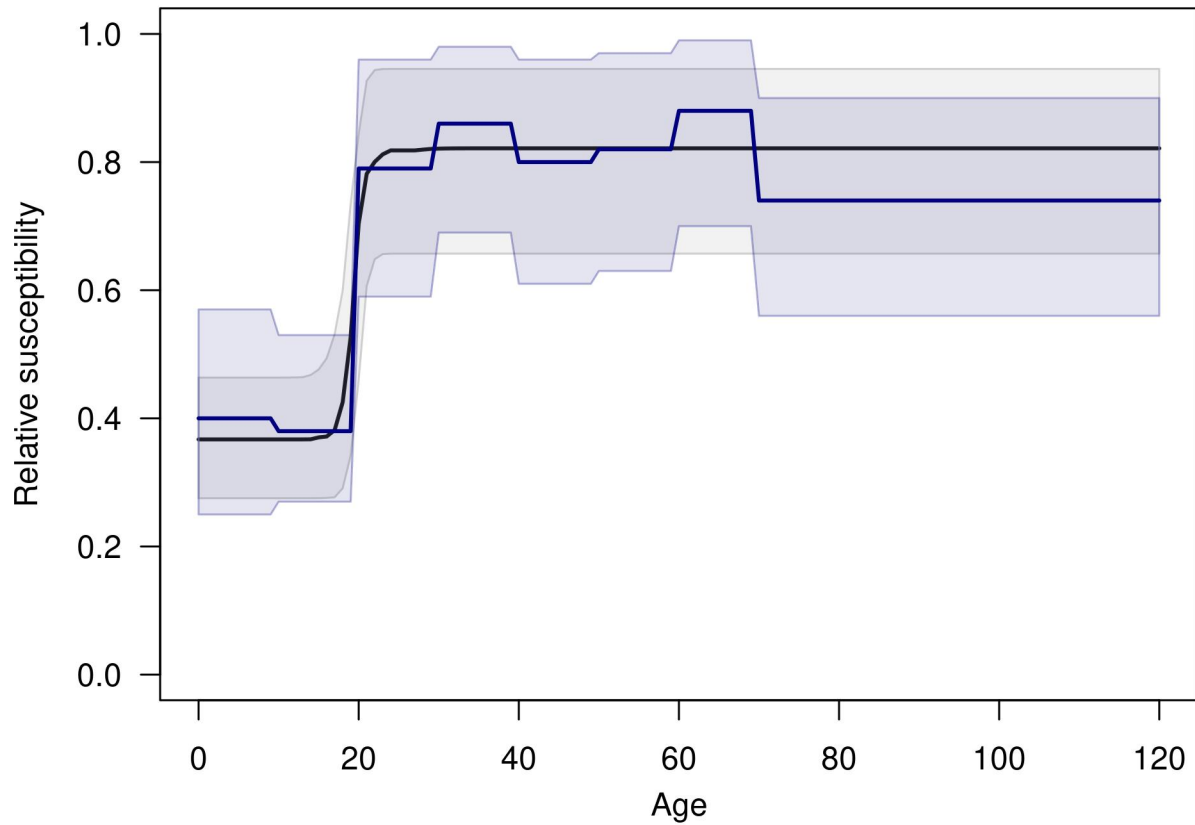


Figure S2. Susceptibility to SARS-CoV-2 infection by age. The black line shows the median of the estimated curve of susceptibility by age, which took the form of a modified logistic function defined by four parameters: minimum, maximum, inflection point, and slope. The gray band represents the 95% credible interval. Navy lines show estimates from Davies et al. [19] that were used to inform our estimates.

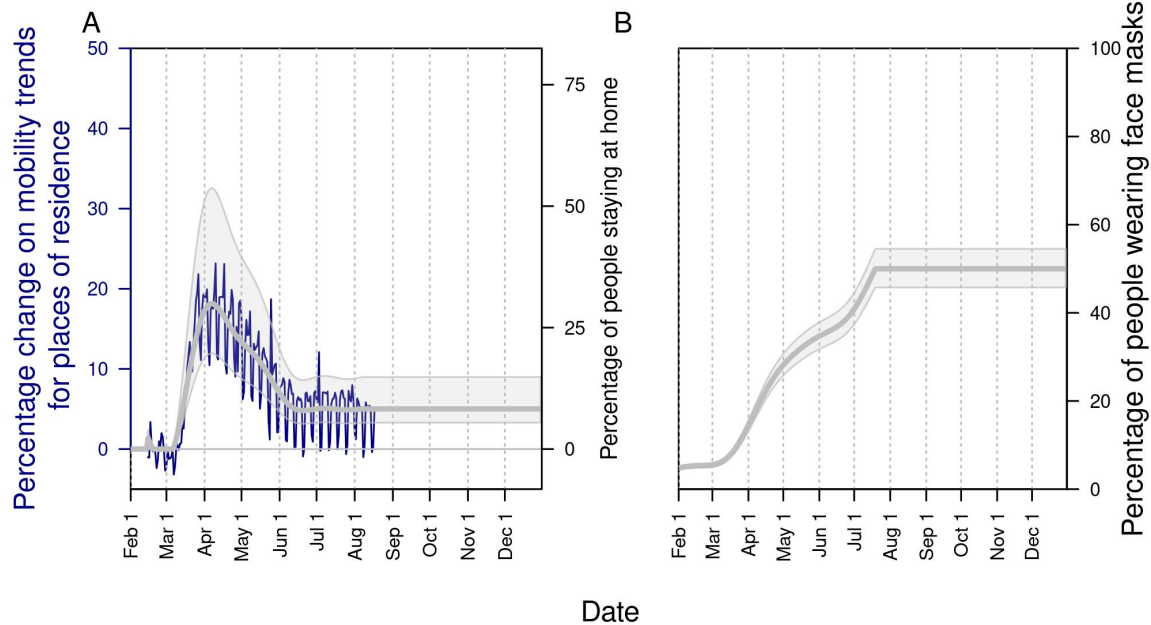


Figure S3. Changes in A) mobility patterns over time and B) face-mask adherence in the community as a whole. In A, the gray line shows the fitted pattern for the Google mobility index related to residential locations (navy line). Adherence to shelter-in-place in the model follows the same trend, but with its magnitude estimated through the model calibration process. In B, the gray line is informed by fitting to Google search data on “face mask” and assuming that values plateau from July 19 onward at a value informed by survey data [47, 48]

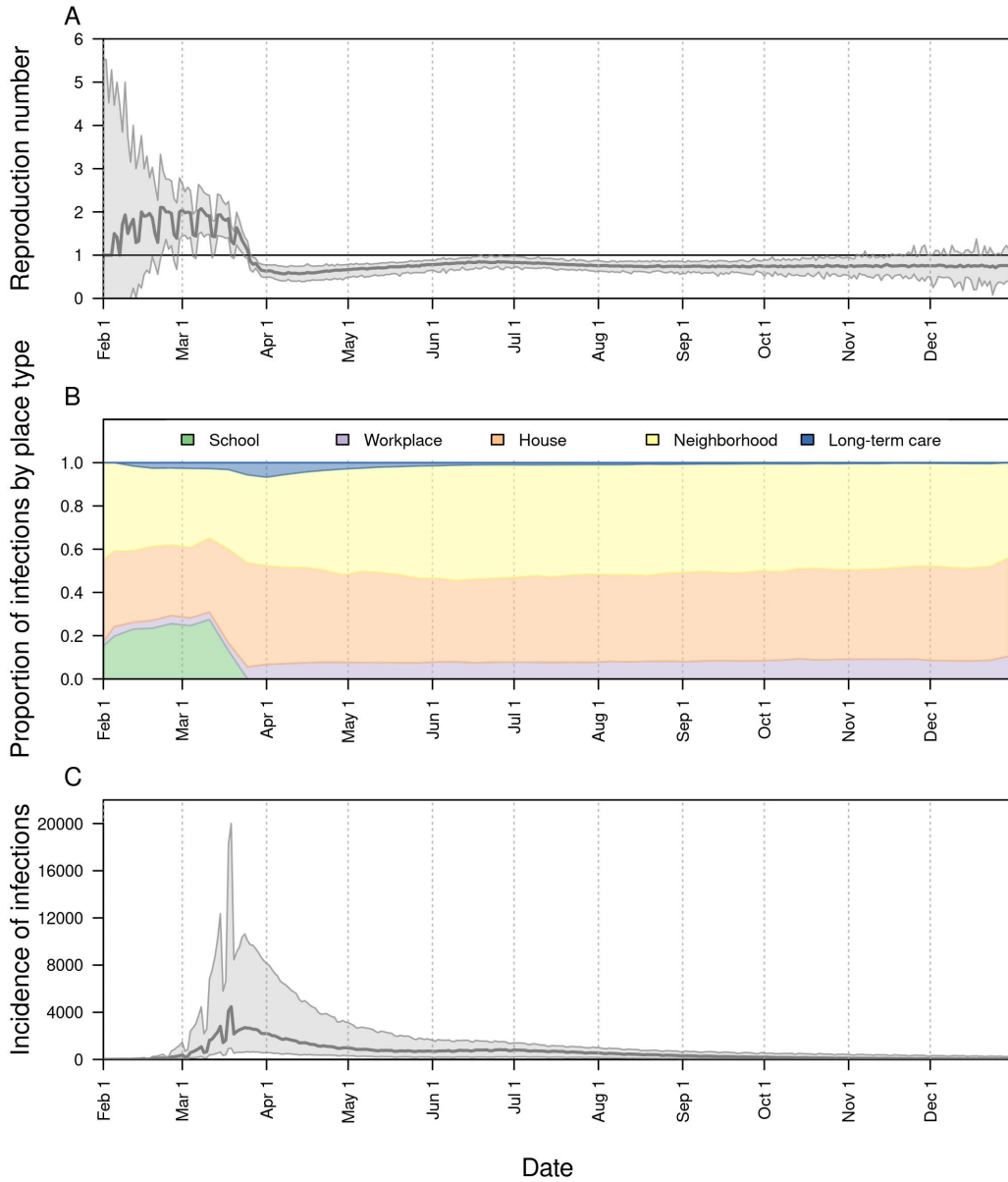


Figure S4. The impact of remote instruction in schools in Indiana on: A) the reproduction number, $R(t)$, over time; B) the proportion of infections acquired in different location types over time; and C) the daily incidence of infection over time. In A and C, the line represents the median, and the shaded region represents the 50% posterior predictive interval.

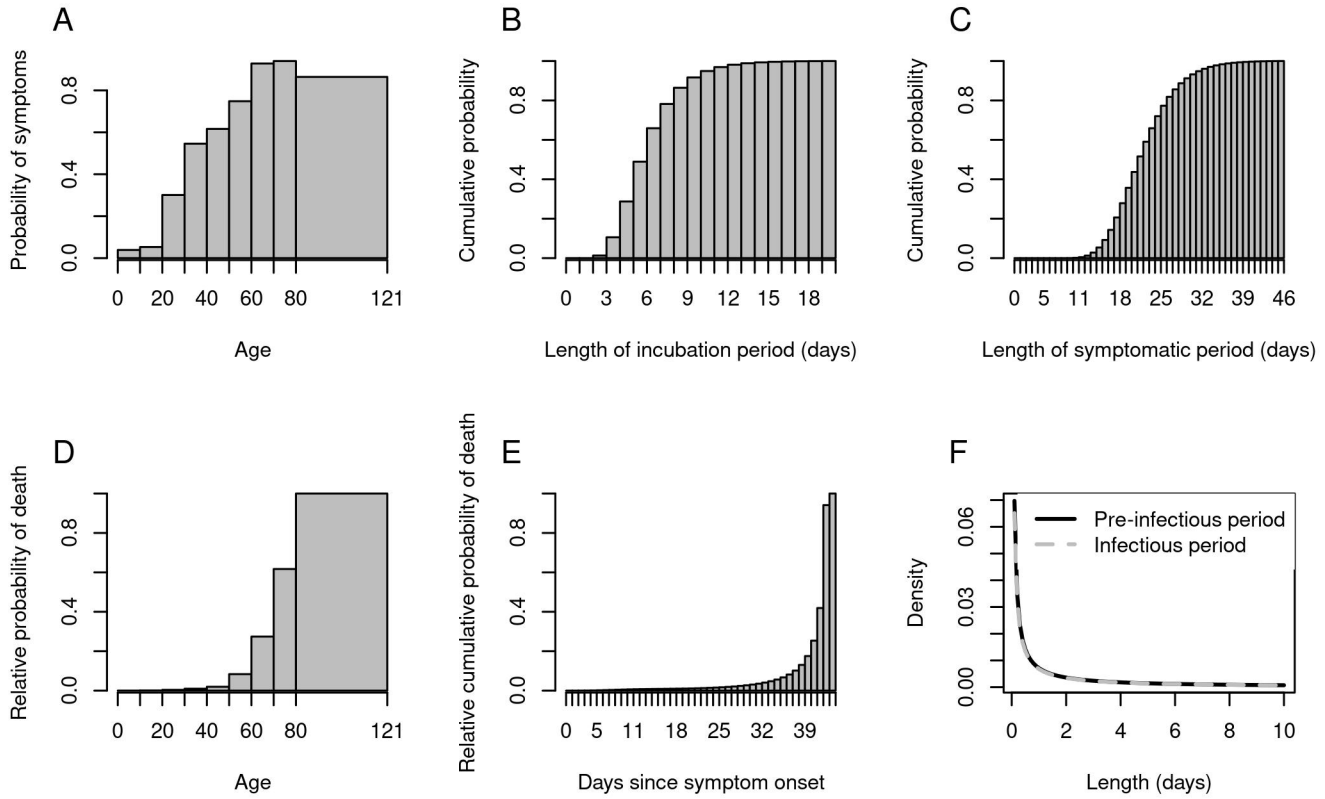


Figure S5. Distributions for parameters in the model. The probability of death is a product of the age-stratified relative probability of death and the daily relative probability of death, conditional on the individual still having symptoms by that day.

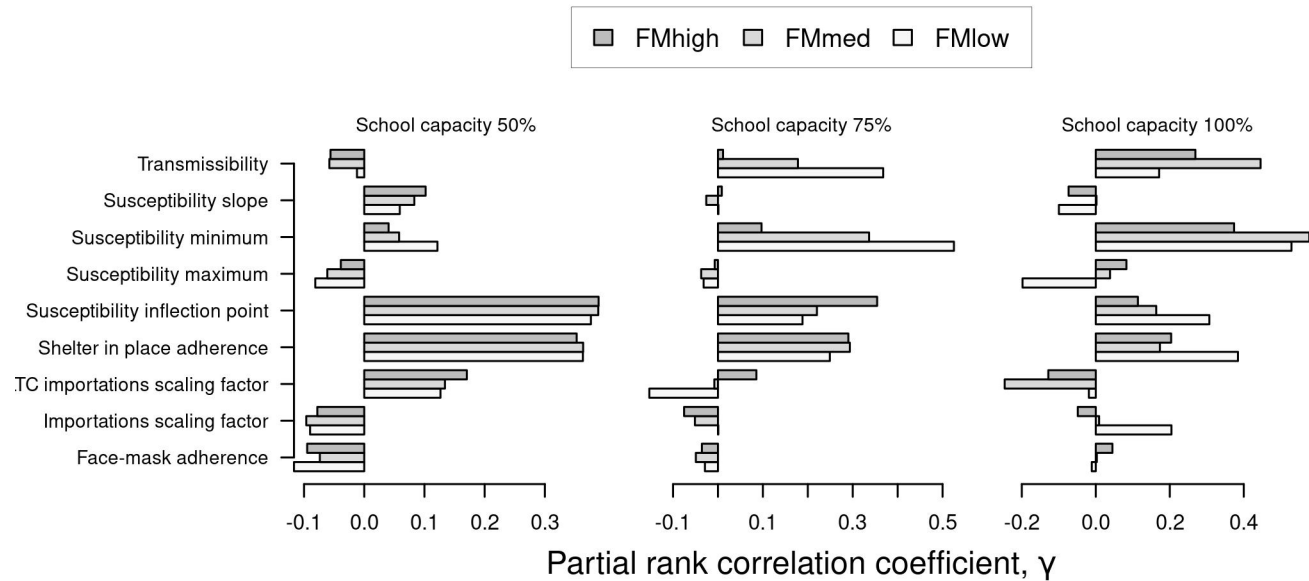


Figure S6. Sensitivity analysis of cumulative infections statewide between August 24 and December 31 to variation in the model's nine parameters. Bars indicate values of the partial rank correlation coefficient. Results are presented separately by school operating capacity (panels) and face-mask adherence in schools (gray shading).

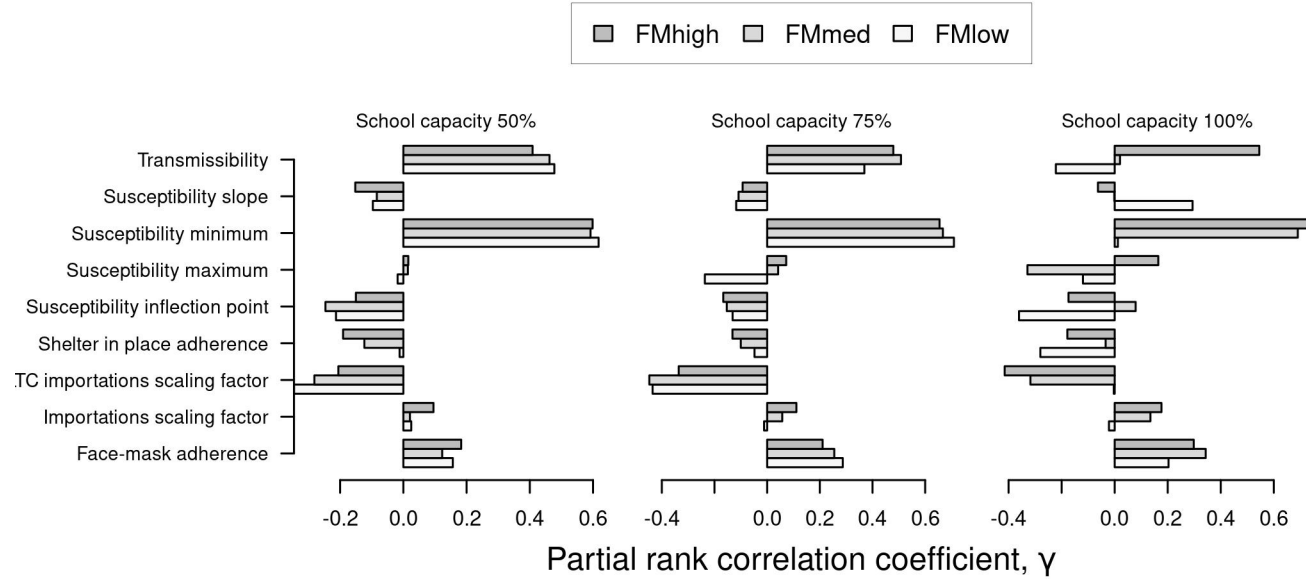


Figure S7. Sensitivity analysis of the proportion of infections acquired in schools between August 24 and December 31 to variation in the model's nine parameters. Bars indicate values of the partial rank correlation coefficient. Results are presented separately by school operating capacity (panels) and face-mask adherence in schools (gray shading).

Capacity	Facemask	Cumulative infections	Cumulative deaths
0.50	Low	1.5 (1.4-1.6)	1.2 (1.1-1.2)
0.50	Med	1.3 (1.2-1.3)	1.1 (1.0-1.1)
0.50	High	1.1 (1.1-1.2)	1.0 (1.0-1.1)
0.75	Low	10.9 (10.3-11.6)	2.6 (2.5-2.8)
0.75	Med	2.8 (2.6-3.0)	1.5 (1.4-1.6)
0.75	High	1.4 (1.3-1.5)	1.2 (1.1-1.2)
1.00	Low	81.8 (78.3-85.7)	13.4 (12.8-14.0)
1.00	Med	29.5 (27.9-31.3)	5.0 (4.8-5.2)
1.00	High	3.0 (2.8-3.1)	1.5 (1.5-1.6)

Table S1. Proportional increase in risk for the overall population of Indiana under alternative scenarios about school operating capacity and face-mask adherence in schools. We define the proportional increase in risk as the ratio of the cumulative number of events (infections or deaths) between August 24 and December 31 under the scenario indicated by the left two columns as compared to a scenario in which schools operate remotely.

Capacity	Facemask	Student infections	Student symptoms
0.50	Low	3.0 (2.8-3.1)	2.7 (2.5-2.8)
0.50	Med	2.0 (1.9-2.1)	1.8 (1.7-1.9)
0.50	High	1.4 (1.4-1.5)	1.3 (1.3-1.4)
0.75	Low	55.3 (52.2-58.5)	43.4 (41.0-46.1)
0.75	Med	9.2 (8.6-9.7)	7.8 (7.3-8.2)
0.75	High	2.6 (2.4-2.7)	2.3 (2.2-2.5)
1.00	Low	470.9 (451.6-491.9)	405.2 (388.3-422.1)
1.00	Med	165.1 (156.4-174.2)	132.2 (125.3-139.7)
1.00	High	9.7 (9.1-10.3)	8.2 (7.7-8.7)

Table S2. Proportional increase in risk for students under alternative scenarios about school operating capacity and face-mask adherence in schools. We define the proportional increase in risk as the ratio of the cumulative number of events (infections or symptomatic infections) between August 24 and December 31 under the scenario indicated by the left two columns as compared to a scenario in which schools operate remotely.

Capacity	Facemask	Teacher infections	Teacher symptoms	Teacher deaths
0.50	Low	2.0 (1.8-2.1)	1.9 (1.8-2.0)	1.7 (1.6-1.9)
0.50	Med	1.5 (1.4-1.6)	1.5 (1.4-1.6)	1.5 (1.4-1.6)
0.50	High	1.3 (1.2-1.4)	1.3 (1.2-1.4)	1.3 (1.2-1.4)
0.75	Low	24.8 (23.1-26.6)	22.0 (20.6-23.4)	15.8 (14.6-17.2)
0.75	Med	5.3 (4.9-5.7)	5.0 (4.7-5.4)	4.7 (4.3-5.2)
0.75	High	2.1 (1.9-2.2)	2.1 (1.9-2.2)	1.8 (1.6-1.9)
1.00	Low	229.2 (218.5-240.4)	229.5 (218.7-240.6)	227.9 (212.0-244.0)
1.00	Med	83.5 (79.1-88.4)	76.7 (72.2-81.2)	58.5 (54.1-63.2)
1.00	High	6.8 (6.3-7.3)	6.5 (6.0-7.0)	6.1 (5.7-6.7)

Table S3. Proportional increase in risk for teachers under alternative scenarios about school operating capacity and face-mask adherence in schools. We define the proportional increase in risk as the ratio of the cumulative number of events (infections, symptomatic infections, or deaths) between August 24 and December 31 under the scenario indicated by the left two columns as compared to a scenario in which schools operate remotely.

Capacity	Facemask	Family infections	Family symptoms	Family deaths
0.50	Low	3.1 (2.9-3.3)	2.9 (2.8-3.1)	2.2 (2.0-2.4)
0.50	Med	2.1 (1.9-2.2)	2.0 (1.9-2.1)	1.6 (1.5-1.7)
0.50	High	1.5 (1.4-1.6)	1.4 (1.4-1.5)	1.4 (1.3-1.5)
0.75	Low	53.0 (49.9-56.2)	44.1 (41.7-47.1)	20.8 (19.3-22.5)
0.75	Med	9.4 (8.9-10.1)	8.5 (7.9-9.0)	5.6 (5.2-6.0)
0.75	High	2.7 (2.6-2.9)	2.6 (2.5-2.8)	2.2 (2.1-2.4)
1.00	Low	459.3 (440.3-478.8)	429.6 (412.4-450.3)	267.0 (252.5-283.5)
1.00	Med	156.8 (148.4-166.1)	133.7 (126.3-141.1)	63.7 (59.5-67.9)
1.00	High	10.0 (9.5-10.7)	9.0 (8.5-9.5)	6.1 (5.7-6.6)

Table S4. Proportional increase in risk for family members of students and teachers under alternative scenarios about school operating capacity and face-mask adherence in schools. We define the proportional increase in risk as the ratio of the cumulative number of events (infections, symptomatic infections, or deaths) between August 24 and December 31 under the scenario indicated by the left two columns as compared to a scenario in which schools operate remotely.

Capacity	Facemask	Cumulative infections	Cumulative deaths
0.50	Low	0.01 (0.01-0.01)	0.05 (0.05-0.05)
0.50	Med	0.01 (0.01-0.01)	0.05 (0.04-0.05)
0.50	High	0.01 (0.01-0.01)	0.04 (0.04-0.05)
0.75	Low	0.10 (0.09-0.10)	0.11 (0.11-0.11)
0.75	Med	0.02 (0.02-0.03)	0.06 (0.06-0.06)
0.75	High	0.01 (0.01-0.01)	0.05 (0.05-0.05)
1.00	Low	0.72 (0.71-0.73)	0.56 (0.54-0.57)
1.00	Med	0.26 (0.25-0.27)	0.21 (0.20-0.22)
1.00	High	0.03 (0.03-0.03)	0.06 (0.06-0.07)

Table S5. Overall proportional reduction in risk for the overall population of Indiana under alternative scenarios about school operating capacity and face-mask adherence in schools. We define the proportional reduction in risk as the ratio of the cumulative number of events (infections or deaths) between August 24 and December 31 under the scenario indicated by the left two columns as compared to a scenario in which schools operate at full capacity and without face masks.

Capacity	Facemask	Student infections	Student symptoms
0.50	Low	0.005 (0.004-0.005)	0.005 (0.004-0.005)
0.50	Med	0.003 (0.003-0.003)	0.003 (0.003-0.003)
0.50	High	0.002 (0.002-0.002)	0.002 (0.002-0.002)
0.75	Low	0.085 (0.081-0.088)	0.075 (0.072-0.078)
0.75	Med	0.014 (0.013-0.015)	0.013 (0.013-0.014)
0.75	High	0.004 (0.004-0.004)	0.004 (0.004-0.004)
1.00	Low	0.720 (0.709-0.730)	0.699 (0.688-0.710)
1.00	Med	0.253 (0.244-0.263)	0.228 (0.219-0.236)
1.00	High	0.015 (0.014-0.015)	0.014 (0.014-0.015)

Table S6. Proportional reduction in risk for students under alternative scenarios about school operating capacity and face-mask adherence in schools. We define the proportional reduction in risk as the ratio of the cumulative number of events (infections or symptomatic infections) between August 24 and December 31 under the scenario indicated by the left two columns as compared to a scenario in which schools operate at full capacity and without face masks.

Capacity	Facemask	Teacher infections	Teacher symptoms	Teacher deaths
0.50	Low	0.006 (0.006-0.007)	0.006 (0.005-0.006)	0.004 (0.004-0.004)
0.50	Med	0.005 (0.005-0.005)	0.005 (0.004-0.005)	0.004 (0.003-0.004)
0.50	High	0.004 (0.004-0.004)	0.004 (0.004-0.004)	0.003 (0.003-0.003)
0.75	Low	0.079 (0.075-0.083)	0.067 (0.064-0.070)	0.038 (0.036-0.040)
0.75	Med	0.017 (0.016-0.018)	0.015 (0.014-0.016)	0.011 (0.011-0.012)
0.75	High	0.007 (0.006-0.007)	0.006 (0.006-0.007)	0.004 (0.004-0.005)
1.00	Low	0.727 (0.719-0.737)	0.698 (0.687-0.708)	0.553 (0.539-0.564)
1.00	Med	0.265 (0.255-0.275)	0.234 (0.225-0.243)	0.142 (0.136-0.148)
1.00	High	0.022 (0.020-0.023)	0.020 (0.019-0.021)	0.015 (0.014-0.016)

Table S7. Proportional reduction in risk for teachers under alternative scenarios about school operating capacity and face-mask adherence in schools. We define the proportional reduction in risk as the ratio of the cumulative number of events (infections, symptomatic infections, or deaths) between August 24 and December 31 under the scenario indicated by the left two columns as compared to a scenario in which schools operate at full capacity and without face masks.

Capacity	Facemask	Family infections	Family symptoms	Family deaths
0.50	Low	0.005 (0.005-0.005)	0.005 (0.004-0.005)	0.004 (0.004-0.005)
0.50	Med	0.003 (0.003-0.003)	0.003 (0.003-0.003)	0.003 (0.003-0.003)
0.50	High	0.002 (0.002-0.002)	0.002 (0.002-0.002)	0.003 (0.003-0.003)
0.75	Low	0.081 (0.078-0.085)	0.069 (0.066-0.073)	0.042 (0.039-0.044)
0.75	Med	0.015 (0.014-0.015)	0.013 (0.013-0.014)	0.011 (0.011-0.012)
0.75	High	0.004 (0.004-0.004)	0.004 (0.004-0.004)	0.004 (0.004-0.005)
1.00	Low	0.705 (0.694-0.716)	0.673 (0.661-0.685)	0.533 (0.520-0.547)
1.00	Med	0.241 (0.231-0.251)	0.210 (0.202-0.218)	0.128 (0.122-0.133)
1.00	High	0.015 (0.015-0.016)	0.014 (0.013-0.015)	0.012 (0.012-0.013)

Table S8. Proportional reduction in risk for family members of students and teachers under alternative scenarios about school operating capacity and face-mask adherence in schools. We define the proportional reduction in risk as the ratio of the cumulative number of events (infections or deaths) between August 24 and December 31 under the scenario indicated by the left two columns as compared to a scenario in which schools operate at full capacity and without face masks.

Parameter	Value
Importations scaling factor	1.118 (95% CrI: 0.654-1.456)
Susceptibility slope	2.502 (95% CrI: 0.733-3.369)
Susceptibility minimum	0.401 (95% CrI: 0.275-0.437)
Susceptibility inflection point	19.648 (95% CrI: 17.644-20.548)
Susceptibility maximum	0.821 (95% CrI: 0.647-0.946)
Shelter in place adherence	0.382 (95% CrI: 0.252-0.687)
Face-mask adherence	0.500 (95% CrI: 0.458-0.545)
LTC importations scaling factor	0.046 (95% CrI: 0.007-0.093)
Transmissibility	0.641 (95% CrI: 0.546-0.965)
Probability of symptoms Age	Fig. S5A
Incubation period	Fig. S5B
Symptomatic period	Fig. S5C
Probability of death Age	Fig. S5D
Probability of death after symptom onset	Fig. S5E
Pre-infectious period	meanlog = 23.7, sdlog = 50 (Fig. S5F)
Infectious period	meanlog = 33.8, sdlog = 43.1 (Fig. S5F)
Adjusted odds ratio for face-mask efficacy	0.15[31]

Table S9. List of model parameters. The first nine were estimated through the model calibration process, and the subsequent seven were assumed based on the literature, as described in the Methods. Values of the first nine parameters reflect marginal posterior estimates.